

## Water-Templated Transmembrane Nanopores from Shape-Persistent Oligocholate Macrocycles

Hongkwan Cho, Lakmini Widanapathirana, and Yan Zhao\*

Department of Chemistry, Iowa State University, Ames, Iowa 50011-3111, United States

Received October 7, 2010; E-mail: zhaoy@iastate.edu

**Abstract:** Hydrophobic interactions normally are not considered a major driving force for self-assembling in a hydrophobic environment. When macrocyclic oligocholates were placed within lipid membranes, however, the macrocycles pulled water molecules from the aqueous phase into their hydrophilic internal cavities. These water molecules had strong tendencies to aggregate in a hydrophobic environment and templated the macrocycles to self-assemble into transmembrane nanopores. This counterintuitive hydrophobic effect resulted in some highly unusual transport behavior. Cholesterol normally increases the hydrophobicity of lipid membranes and makes them less permeable to hydrophilic molecules. The permeability of glucose across the oligocholate-containing membranes, however, increased significantly upon the inclusion of cholesterol. Large hydrophilic molecules tend to have difficulty traversing a hydrophobic barrier. The cyclic cholate tetramer, however, was more effective at permeating maltotriose than glucose.

### Introduction

Channels and pores are used in biology to permeate ions and molecules across membranes. In addition to their important roles in signaling, metabolism, and bacterial or viral infection, channels and pores enable design of novel sensors for both small and large molecules.<sup>1</sup> Pore-forming proteins, for example, have shown great promises in the single-molecule detection of RNAs and DNAs.<sup>2</sup>

Although synthetic pores have the advantage of being less expensive and less prone to denaturation than their protein counterparts, development of nanometer-sized synthetic pores has been a difficult challenge.<sup>3</sup> Ghadiri et al. prepared cyclic peptides that self-assembled into pores large enough for glucose and glutamic acid to pass through.<sup>4</sup> Matile and co-workers, in a series of seminal work, reported nanometer-sized  $\beta$ -barrel pores through self-assembly of oligo(phenylene) derivatives<sup>5</sup> and demonstrated their applications in sensing<sup>5b</sup> and catalysis.<sup>5c</sup>

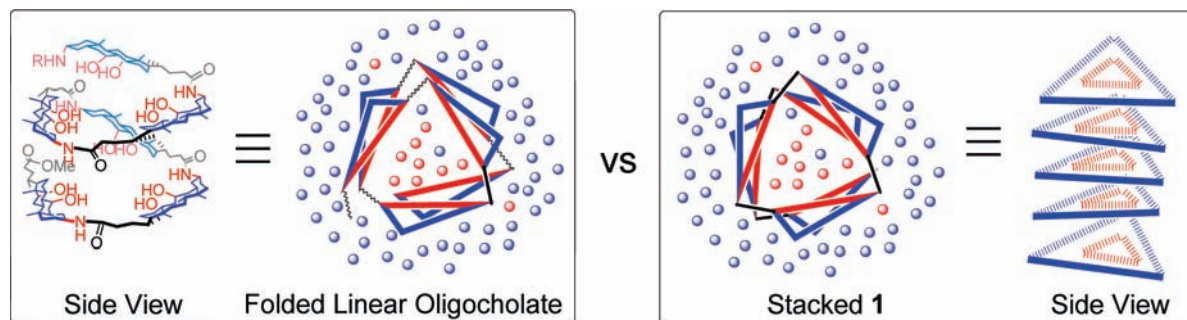
More recently, Satake and Kobuke prepared nanosized pores based on porphyrin supramolecules.<sup>6</sup> Gong et al. described pores ca. 0.8 nm in diameter through the  $\pi$ - $\pi$  interactions of aromatic heterocycles.<sup>7</sup> In addition, Fyles<sup>8</sup> and Davis<sup>9</sup> used amine-Pd(II) and guanosine quartets, respectively, to construct highly conducting channels consistent with nanometered pore sizes.

A big challenge in creating nanometer-sized pores within the lipid bilayers is to keep the pore from collapsing. For this reason, although chemists have made tremendous progress in the design and synthesis of artificial ion channels,<sup>10</sup> the building blocks involved (e.g., crown ethers and open chain compounds) typically are not amenable to nanopore formation. Despite the advancement made in synthetic nanopores, only limited pore-forming mechanisms exist currently. The majority of synthetic nanopores reported so far relied on either hydrogen-bonding<sup>4,5,9</sup> or metal-ligand coordination<sup>6,8</sup> for stability.

Herein, we report synthetic nanopores driven by *hydrophobic* interactions—a very different mechanism of pore formation from common biological and synthetic examples. The novelty of the approach lies in the counterintuitive design. Normally, if the environment (i.e., lipid bilayers) is hydrophobic, hydrophobic interactions are not expected to contribute significantly to a supramolecular synthesis. The self-assembled pores displayed

- (1) Kasianowicz, J. J.; Robertson, J. W. F.; Chan, E. R.; Reiner, J. E.; Stanford, V. M. *Annu. Rev. Anal. Chem.* **2008**, *1*, 737–766.
- (2) (a) Kasianowicz, J. J.; Brandin, E.; Branton, D.; Deamer, D. W. *Proc. Natl. Acad. Sci. U.S.A.* **1996**, *93*, 13770–13773. (b) Akeson, M.; Branton, D.; Kasianowicz, J. J.; Brandin, E.; Deamer, D. W. *Biophys. J.* **1999**, *77*, 3227–3233. (c) Meller, A.; Nivon, L.; Brandin, E.; Golovchenko, J.; Branton, D. *Proc. Natl. Acad. Sci. U.S.A.* **2000**, *97*, 1079–1084. (d) Vercoutere, W.; Winters-Hilt, S.; Olsen, H.; Deamer, D.; Haussler, D.; Akeson, M. *Nat. Biotechnol.* **2001**, *19*, 248–252. (e) Howorka, S.; Cheley, S.; Bayley, H. *Nat. Biotechnol.* **2001**, *19*, 636–639. (f) Clarke, J.; Wu, H. C.; Jayasinghe, L.; Patel, A.; Reid, S.; Bayley, H. *Nat. Biotechnol.* **2009**, *4*, 265–270.
- (3) (a) Matile, S.; Som, A.; Sordé, N. *Tetrahedron* **2004**, *60*, 6405–6435. (b) Sisson, A. L.; Shah, M. R.; Bhosale, S.; Matile, S. *Chem. Soc. Rev.* **2006**, *35*, 1269–1286.
- (4) (a) Granja, J. R.; Ghadiri, M. R. *J. Am. Chem. Soc.* **1994**, *116*, 10785–10786. (b) Sánchez-Quesada, J.; Kim, H. S.; Ghadiri, M. R. *Angew. Chem., Int. Ed.* **2001**, *40*, 2503–2506.
- (5) (a) Sakai, N.; Mareda, J.; Matile, S. *Acc. Chem. Res.* **2005**, *38*, 79–87. (b) Das, G.; Talukdar, P.; Matile, S. *Science* **2002**, *298*, 1600–1602. (c) Sakai, N.; Sordé, N.; Matile, S. *J. Am. Chem. Soc.* **2003**, *125*, 7776–7777.

- (6) Satake, A.; Yamamura, M.; Oda, M.; Kobuke, Y. *J. Am. Chem. Soc.* **2008**, *130*, 6314–6315.
- (7) Helsel, A. J.; Brown, A. L.; Yamato, K.; Feng, W.; Yuan, L. H.; Clements, A. J.; Harding, S. V.; Szabo, G.; Shao, Z. F.; Gong, B. *J. Am. Chem. Soc.* **2008**, *130*, 15784–15785.
- (8) Fyles, T. M.; Tong, C. C. *New J. Chem.* **2007**, *31*, 655–661.
- (9) Ma, L.; Melegari, M.; Colombini, M.; Davis, J. T. *J. Am. Chem. Soc.* **2008**, *130*, 2938–2939.
- (10) (a) Gokel, G. W.; Mukhopadhyay, A. *Chem. Soc. Rev.* **2001**, *30*, 274–286. (b) Fyles, T. M. *Chem. Soc. Rev.* **2007**, *36*, 335–347. (c) Koert, U.; Al-Momani, L.; Pfeifer, J. R. *Synthesis-Stuttgart* **2004**, 1129–1146. (d) Gokel, G. W.; Murillo, O. *Acc. Chem. Res.* **1996**, *29*, 425–432. (e) Jung, M.; Kim, H.; Baek, K.; Kim, K. *Angew. Chem., Int. Ed.* **2008**, *47*, 5755–5757. (f) Li, X.; Shen, B.; Yao, X. Q.; Yang, D. *J. Am. Chem. Soc.* **2009**, *131*, 13676–13680.

**Scheme 1.** Schematic Representation of the Solvophobic Driven Folding of a Linear Oligocholate and Aggregation of 1

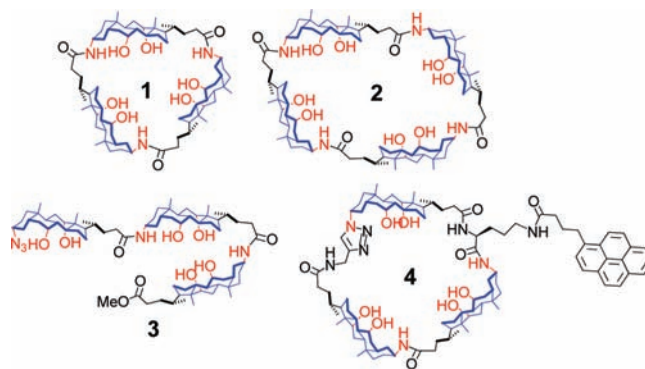
highly unusual behavior as a result of the counterintuitive pore-formation. Cholesterol is known to increase the hydrophobic thickness<sup>11</sup> of lipid bilayers and decrease their fluidity.<sup>12</sup> Yet, the enhanced hydrophobicity caused by cholesterol facilitated the pore formation of the oligocholate macrocycles and increased the permeability of glucose across the membranes. Larger hydrophilic molecules normally have difficulty moving across a hydrophobic barrier. The cyclic cholate tetramer, however, was more effective at permeating maltotriose than glucose.

## Results and Discussion

**Molecular Design.** With a cholesterol-like backbone and facial amphiphilicity, cholic acid derivatives have been used in membrane-related applications including as ion channels<sup>9,13</sup> and molecule<sup>14</sup> or anion transporters.<sup>15</sup> In an effort to prepare conformationally controllable foldamers,<sup>16</sup> we synthesized linear oligomers of facially amphiphilic cholates.<sup>17</sup> In nonpolar solvents (e.g., CCl<sub>4</sub> or hexane/ethyl acetate) containing a small percentage of a polar solvent (e.g., DMSO or MeOH), the oligocholate folds into a helix with a nanometer-sized hydro-

philic inner pore. The polar solvent phase-separates from the bulk into the hydrophilic pore and efficiently solvate the introverted polar groups of the oligocholate (Scheme 1, left).

Since the folded helix has three monomer units per turn,<sup>17a</sup> cyclic tricholate **1** essentially represents the cross section of the folded helix. According to the CPK model, the molecule has a triangular hydrophilic cavity about 1 nm on the side (the N–N distance is ~1.3 nm). Its exterior is completely hydrophobic and fully compatible with lipid membranes. Its rigidity, resulting from both the triangular geometry and the fused steroid backbone, is expected to prevent the inner cavity from collapsing. Note that, although other strategies (e.g., internal charge repulsion)<sup>18</sup> have been used with success, rigidity of the building blocks is a key factor in keeping synthetic nanopores from collapsing.<sup>3–9</sup>



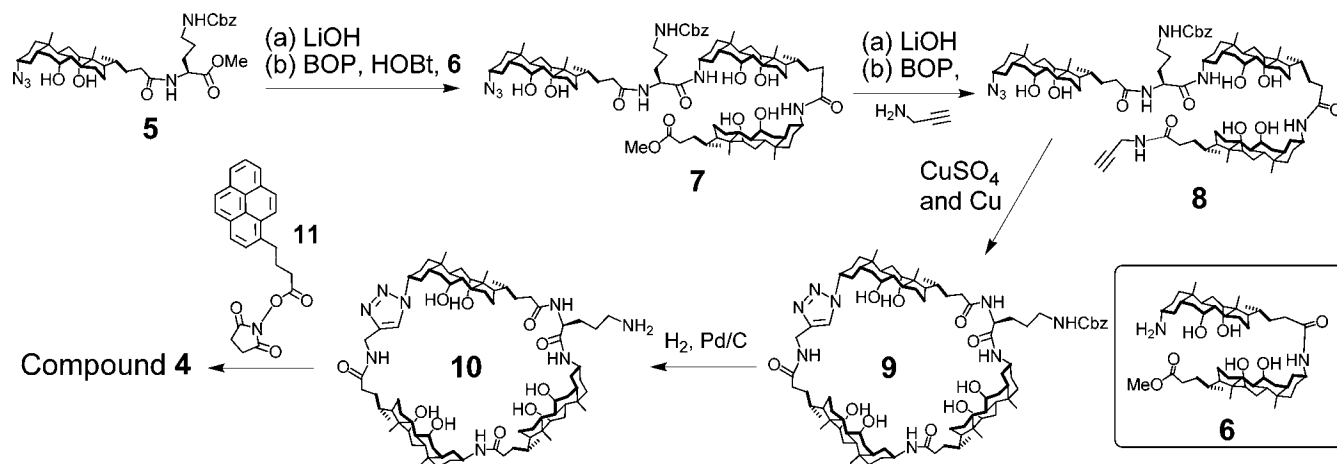
We hypothesized that the same solvophobic driving force in the folding of the linear oligocholates<sup>17</sup> would prompt **1** to stack in the  $z$ -direction (Scheme 1, right). In a largely nonpolar solvent mixture, the polar solvent molecules should phase-separate into the middle of the macrocycle and solvate the inward-facing polar groups. Aggregation also allows these polar solvents to move up and down the polar channel—an entropically favorable process.

In addition to **1**, cyclic tetramer **2** and linear trimer **3** were prepared as control compounds. Compound **4** has a pyrene group on the side chain, allowing us to use fluorescence to probe the self-assembly. Linear oligocholates such as **3** were synthesized through standard amide-coupling reactions.<sup>17a</sup> Cyclization of the corresponding amino/carboxyl-terminated oligocholates yielded compounds **1** and **2** (see the Supporting Information for details). For compound **4**, we took advantage of the azide group at the end of the oligocholates and used the click reaction<sup>19</sup> for the

- (11) Nezil, F. A.; Bloom, M. *Biophys. J.* **1992**, *61*, 1176–1183.  
 (12) Holthuis, J. C. M.; van Meer, G.; Huitema, K. *Mol. Membr. Biol.* **2003**, *20*, 231–241.  
 (13) (a) Bandyopadhyay, P.; Janout, V.; Zhang, L. H.; Sawko, J. A.; Regen, S. L. *J. Am. Chem. Soc.* **2000**, *122*, 12888–12889. (b) Goto, C.; Yamamura, M.; Satake, A.; Kobuke, Y. *J. Am. Chem. Soc.* **2001**, *123*, 12152–12159. (c) Maulucci, N.; De Riccardis, F.; Botta, C. B.; Casapullo, A.; Cressina, E.; Fregonese, M.; Tecilla, P.; Izzo, I. *Chem. Commun.* **2005**, 1354–1356. (d) Wilson, C. P.; Webb, S. J. *Chem. Commun.* **2008**, 4007–4009.  
 (14) (a) Janout, V.; Di Giorgio, C.; Regen, S. L. *J. Am. Chem. Soc.* **2000**, *122*, 2671–2672. (b) Janout, V.; Staina, I. V.; Bandyopadhyay, P.; Regen, S. L. *J. Am. Chem. Soc.* **2001**, *123*, 9926–9927. (c) Janout, V.; Jing, B. W.; Staina, I. V.; Regen, S. L. *J. Am. Chem. Soc.* **2003**, *125*, 4436–4437. (d) Janout, V.; Regen, S. L. *J. Am. Chem. Soc.* **2005**, *127*, 22–23.  
 (15) (a) Koulou, A. V.; Lambert, T. N.; Shukla, R.; Jain, M.; Boon, J. M.; Smith, B. D.; Li, H. Y.; Sheppard, D. N.; Joos, J. B.; Clare, J. P.; Davis, A. P. *Angew. Chem., Int. Ed.* **2003**, *42*, 4931–4933. (b) Whitmarsh, S. D.; Redmond, A. P.; Sgarlata, V.; Davis, A. P. *Chem. Commun.* **2008**, 3669–3671.  
 (16) For several representative reviews, see: (a) Gellman, S. H. *Acc. Chem. Res.* **1998**, *31*, 173–180. (b) Hill, D. J.; Mio, M. J.; Prince, R. B.; Hughes, T. S.; Moore, J. S. *Chem. Rev.* **2001**, *101*, 3893–4012. (c) Hecht, S.; Huc, I. *Foldamers: structure, properties, and applications*; Wiley-VCH: Weinheim, 2007. (d) Cubberley, M. S.; Iverson, B. L. *Curr. Opin. Chem. Biol.* **2001**, *5*, 650–653. (e) Kirshenbaum, K.; Zuckermann, R. N.; Dill, K. A. *Curr. Opin. Struct. Biol.* **1999**, *9*, 530–535. (f) Goodman, C. M.; Choi, S.; Shandler, S.; DeGrado, W. F. *Nat. Chem. Biol.* **2007**, *3*, 252–262. (g) Bautista, A. D.; Craig, C. J.; Harker, E. A.; Schepartz, A. *Curr. Opin. Chem. Biol.* **2007**, *11*, 685–692.  
 (17) (a) Zhao, Y.; Zhong, Z. *J. Am. Chem. Soc.* **2005**, *127*, 17894–17901. (b) Zhao, Y.; Zhong, Z.; Ryu, E. H. *J. Am. Chem. Soc.* **2007**, *129*, 218–225. (c) Cho, H.; Zhao, Y. *J. Am. Chem. Soc.* **2010**, *132*, 9890–9899. (d) Zhao, Y. *J. Org. Chem.* **2009**, *74*, 834–843. (e) Pan, X.; Zhao, Y. *Org. Lett.* **2009**, *11*, 69–72.

- (18) Som, A.; Matile, S. *Chem. Biodiv.* **2005**, *2*, 717–729.

Scheme 2. Synthetic Route for Pyrene-Labeled Macrocyclic 4



cyclization (Scheme 2). The pyrene group was introduced at the side chain of the L-ornithine inserted in between two cholates.

**Glucose Leakage from POPC/POPG LUVs.** An ideal system to test the stacking is the lipid bilayer. The lipid hydrocarbon tails essentially are the nonpolar solvent in Scheme 1 and the assembly of **1** in the  $z$ -direction would create a transmembrane nanopore (Figure 1, C). Because the nanopore is open to bulk water on both ends, the water molecules inside the pore can readily exchange with bulk water. This is very important if the pore-formation is to occur. Because the entropic cost for trapping a single water molecule can be as high as 2 kcal/mol,<sup>20</sup> any partial pore-formation (as in A or B) could be strongly disfavored.

Many macrocycles of bile acids have been reported in the literature.<sup>15b,21</sup> A similar cyclic trimer of a cholate derivative was found to bind monosaccharides.<sup>21a,b</sup> We thus employed the well-established glucose leakage assay to test the pore-formation. Briefly, glucose (300 mM) was first encapsulated within POPC/POPG large unilamellar vesicles (LUVs) and the external glucose was removed by gel filtration. When different amounts of **1** were added to the liposomal solution,<sup>22</sup> the glucose that leaked out was converted by extravesically added hexokinase and ATP to glucose-6-phosphate, which was oxidized by glucose-6-phosphate dehydrogenase while NADP was reduced to NADPH. Because of the fast enzymatic kinetics, the formation of NADPH at 340 nm correlates directly with the rate of glucose efflux.<sup>23</sup>

To our delight, tricholate **1** was highly effective at transporting glucose across lipid membranes (Figure 1S, Supporting Information). The leakage was strongly dependent on its concentration. Glucose efflux was negligible below 0.125  $\mu\text{M}$  of **1**. The leakage showed a noticeable increase at 0.25  $\mu\text{M}$  of the

macrocyclic, but another 2-fold increase in the transporter concentration caused a dramatic increase in leakage—over 90% of glucose leaked out after 60 min.

Because **1** cannot turn its hydrophilic inside out, we did not consider “toroidal pores”, in which amphiphilic molecules (typically surfactants or amphipathic peptides) cause local phase changes in the lipids and produce transient openings in the membrane.<sup>3</sup> We performed the lipid mixing assay and tested the possibility of membrane fusion as a potential cause of leakage,<sup>24</sup> but <10% lipid mixing occurred even at the highest [oligocholates]/[lipid] ratio used in the glucose leakage assay (Figure 1S).<sup>25</sup>

After lipid fusion was excluded as a main cause for leakage, we considered three other possible mechanisms for the glucose efflux, with either the monomer or an aggregate of **1** as the main transporting species. In a carrier- or ferry-based mechanism, a glucose-bound macrocycle (either in the form of A or B shown in Figure 1) migrates from the inner to the outer leaflet of the bilayer, where the guest is released.<sup>26</sup> In a relay mechanism, the guest still has to be bound by A or B but the binding is only transient and the guest hops from one station to another before exiting the bilayer. The third possibility is the hypothesized nanopore, represented by (the idealized) C in Figure 1.

A carrier-based mechanism typically gives a linear relationship between the leakage rate and the monomer concentration<sup>27</sup> but the strong dependence of leakage on the concentration of **1** suggests that its aggregate was the active transporter (vide infra).<sup>3,27</sup> Either B or C would fit such a scenario. To distinguish between the latter two mechanisms, we studied cyclic tetramer **2** and linear trimer **3** in the transport. The difference between **1** and **2** is not just in size but, more importantly, in their rigidity. A triangle cannot change its shape as long as the sides are rigid,

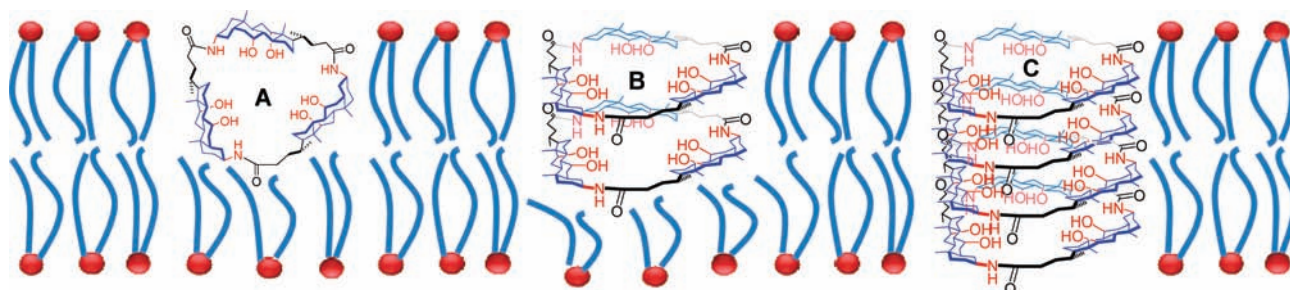
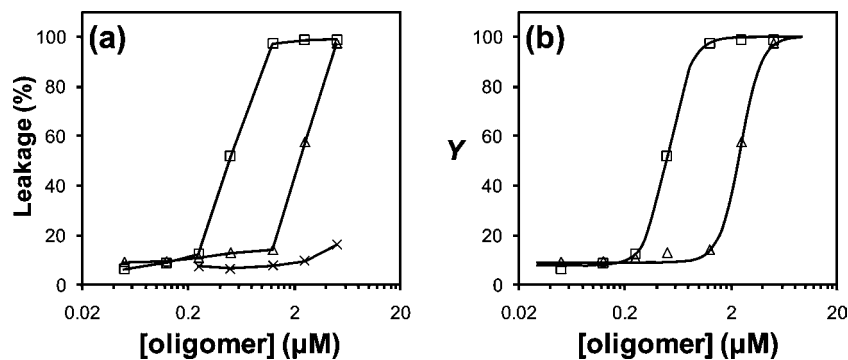


Figure 1. Possible arrangements of cyclic tricholate **1** in a lipid bilayer.



**Figure 2.** (a) Percent leakage of glucose at 30 min from POPC/POPG LUVs as a function of oligocholate concentration for **1** (□), **2** (△), and **3** (×) at ambient temperature. Total concentration of phospholipids was 107 μM. These leakage experiments were typically done in duplicates and the error within the two <10%. (b) Nonlinear least-squares fitting of the leakage data to the Hill equation for **1** (□) and **2** (△). The fraction activity ( $Y$ ) is the percent glucose leakage of the LUVs at 30 min after addition of the oligomers.

but a quadrilateral can bend and twist even if the sides are completely rigid. Thus, stacking and transmembrane pore-formation should be more difficult with **2** than with **1**. Linear trimer **3** should be even less competent, as it has to fold before it can stack to form the pore (assuming the same pore-formation mechanism is involved).

Figure 2a shows the glucose leakage of LUVs at 30 min in the presence of the different oligocholates. The topology of the oligocholates impacted the transport strongly. It took 4–5 times as much **2** as **1**, for example, to leak the same amount of glucose from the LUVs. The general facial amphiphilicity of the cholates clearly was *not* the determining factor, as tetramer **2** contained more cholates than trimer **1** and yet was less effective. The conclusion was further supported by linear trimer **3**, which displayed leakage slightly above the background (6–10%) even at the highest tested concentration. Once the ring structure was removed, the oligocholate completely lost its ability of transport.

The leakage data in Figure 2a suggests high cooperativity among the macrocycles.<sup>3</sup> A common way to analyze the cooperativity of a supramolecular system is through the Hill equation,  $Y = Y_{\text{low}} + (Y_{\text{high}} - Y_{\text{low}}) / [1 + (EC_{50}/c)^n]$ , in which the fractional activity ( $Y$ ) of a supramolecule is related to the monomer concentration ( $c$ ).<sup>28</sup>  $EC_{50}$  is the concentration of the

monomer that produces 50% activity. The Hill coefficient ( $n$ ) indicates both the stability of the self-assembly and the number of monomers in the supramolecule responsible for the activity. A Hill coefficient of  $n > 1$  means that the monomer is the dominant species and yet the supramolecule is responsible for the observed activity.<sup>3b,29</sup>

Significantly, the leakage data fit well to the Hill equation (Figure 2b), yielding a Hill coefficient of  $n = 4.0 \pm 0.3$  for cyclic trimer **1** and  $4.4 \pm 0.5$  for tetramer **2**.<sup>30</sup> Thus, for both macrocycles, the active transporting supramolecule seems to consist of four macrocycles. POPC bilayer is about 2.6 nm in the hydrophobic thickness.<sup>11,31</sup> The cholates are about 0.6–0.7 nm on the side. To the extent that the Hill analysis reflects accurately the assembly process, the active transporting species was most likely a transmembrane pore assembled from four macrocycles.

Comparison of the three possible arrangements of the macrocycle in Figure 1 reveals the reasons for the pore-formation.<sup>32</sup> When a cyclic oligocholate enters the membrane, the introverted hydroxyl/amide groups demand the internal cavity to be filled with water/glucose instead of lipid hydrocarbon. If the macrocycle exists as a monomer (Figure 1, **A**), the entrapped water/glucose would face hydrocarbon at least on one end of the cavity or on both ends if the molecule penetrates deep into the bilayer. The unfavorable hydrophilic–hydrophobic contact can be reduced if the molecules stack on top of one another (**B**), but can be eliminated only if a transmembrane pore (**C**) is formed. In the last case, not only is water–hydrocarbon contact eliminated on both ends of the cavity for all the macrocycles involved, but also the water molecules

- (19) (a) Rostovtsev, V. V.; Green, L. G.; Fokin, V. V.; Sharpless, K. B. *Angew. Chem., Int. Ed.* **2002**, *41*, 2596–2599. (b) Kolb, H. C.; Finn, M. G.; Sharpless, K. B. *Angew. Chem., Int. Ed.* **2001**, *40*, 2004–2021.
- (20) Dunitz, J. D. *Science* **1994**, *264*, 670.
- (21) (a) Bonar Law, R. P.; Davis, A. P.; Murray, B. A. *Angew. Chem., Int. Ed. Engl.* **1990**, *29*, 1407–1408. (b) Davis, A. P.; Walsh, J. J. *Chem. Commun.* **1996**, 449–451. (c) Brotherhood, P. R.; Davis, A. P. *Chem. Soc. Rev.* **2010**, *39*, 3633–3647. (d) Brady, P. A.; Bonar Law, R. P.; Rowan, S. J.; Suckling, C. J.; Sanders, J. K. M. *Chem. Commun.* **1996**, 319–320. (e) Ghosh, S.; Choudhury, A. R.; Row, T. N. G.; Maitra, U. *Org. Lett.* **2005**, *7*, 1441–1444.
- (22) In our leakage assay, we added **1** to the liposomal solution as a solution of DMSO (10–20 μL). The amount of DMSO was tested and found to have negligible effects on the LUVs.
- (23) Kinsky, S. C.; Haxby, J. A.; Zopf, D. A.; Alving, C. R.; Kinsky, C. B. *Biochemistry* **1969**, *8*, 4149–4158.
- (24) Struck, D. K.; Hoekstra, D.; Pagano, R. E. *Biochemistry* **1981**, *20*, 4093–4099.
- (25) The 100% end point in a fusion assay can be measured either after a surfactant such as Triton X-100 is added to destroy the liposomes or through a “mock” fusion product (i.e., liposomes whose probe density corresponds to that of completely fused liposomes). Although the Triton method gave similar results, we mainly used the second approach for our fusion experiments because Triton X-100 impacts the quantum yield of NBD. For a discussion on different lipid-mixing fusion assays, see: Hoekstra, D.; Düzgüneş, N. *Methods Enzymol.* **1993**, *220*, 15–32.
- (26) Smith, B. D.; Lambert, T. N. *Chem. Commun.* **2003**, 2261–2268.

- (27) (a) Deng, G.; Merritt, M.; Yamashita, K.; Janout, V.; Sadownik, A.; Regen, S. L. *J. Am. Chem. Soc.* **1996**, *118*, 3307–3308. (b) Merritt, M.; Lanier, M.; Deng, G.; Regen, S. L. *J. Am. Chem. Soc.* **1998**, *120*, 8494–8501.
- (28) Hille, B. *Ionic channels of excitable membranes*; 2nd ed.; Sinauer Associates: Sunderland, MA, 1992.
- (29) Litvinchuk, S.; Bollot, G.; Mareda, J.; Som, A.; Ronan, D.; Shah, M. R.; Perrotet, P.; Sakai, N.; Matile, S. *J. Am. Chem. Soc.* **2004**, *126*, 10067–10075.
- (30) Leakage at 60 min gave similar results, but the curve fitting to the Hill equation was less certain because the data points clustered at either very high ( $Y > 90\%$ ) or very low ( $Y < 30\%$ ) leakage.
- (31) Lewis, B. A.; Engelman, D. M. *J. Mol. Biol.* **1983**, *166*, 203–210.
- (32) Hydrogen bonds among the amides along the pore axis are unlikely to contribute significantly because the amides are exposed to water molecules inside the pore. Also, the steroid backbone is large on the amino end and small near the carboxy tail. The geometry of the macrocycle thus prohibits close contact of the amide bonds in the  $z$ -direction.

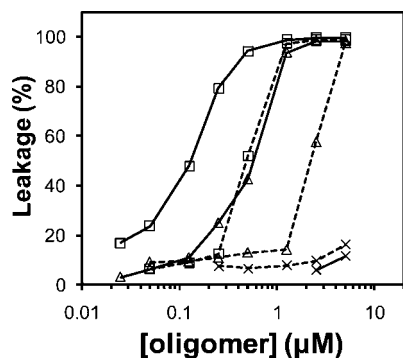


**Figure 3.** Percent leakage of glucose at 30 min from POPC/POPG LUVs as a function of oligocholate concentration for **1** (□), **2** (△), and **3** (×) at ambient temperature. The data points connected by solid lines are for the LUVs containing 30 mol % of cholesterol, whereas those connected by dotted lines are for the LUVs without cholesterol, taken from Figure 2. Total concentration of phospholipids was 107  $\mu\text{M}$ .

inside the macrocycle are no longer confined in a nanospace. The water molecules within the pore can solvate all the polar groups on the inner wall and yet still exchange with the bulk water rapidly. The exchange of water clearly will be more difficult if one or both ends of the cavity are capped by hydrocarbon, as in **A** or **B**.

#### Effect of Cholesterol on the Oligocholate-Induced Leakage.

To gain additional evidence for the pore-formation, we included 30 mol % of cholesterol in the lipid formulation. Cholesterol is known to increase the hydrophobic thickness<sup>11</sup> of POPC bilayer and decrease its fluidity.<sup>12</sup> Cholesterol-containing bilayers are much less permeable to hydrophilic molecules, including glucose and glycerol.<sup>33</sup>

Notably, glucose leakage became *significantly faster* when the bilayers contained 30 mol % of cholesterol (Figure 3). The data points connected by solid lines represent leakage from the cholesterol-containing LUVs and those by dotted lines are from the cholesterol-free ones. Both the trimer and the tetramer clearly benefited from cholesterol. The concentration of the transporter that causes 50% leakage at 30 min (i.e.,  $\text{EC}_{50}$ ) for the trimer went from  $\sim 0.5$  to  $\sim 0.1$   $\mu\text{M}$  upon cholesterol inclusion; that for the tetramer decreased from  $\sim 2.4$  to  $\sim 0.5$   $\mu\text{M}$ . The cyclic topology remained critical to the transport, as the linear trimer (×) was completely unaffected by the cholesterol added.

These results strongly support the pore-formation mechanism. Because cholesterol makes the membrane more hydrophobic,<sup>33</sup> the hydrophobic driving force mentioned above is higher for the stacking of the macrocycles. Cholesterol is able to induce lateral heterogeneity in lipid membranes.<sup>34</sup> If cholesterol-rich and -deficient domains exist, pore formation should be easier if the macrocycle phase-separates into one domain. Given that cholic acid is a metabolite of cholesterol, **1** and **2** are highly likely to fall into cholesterol-rich domains.

#### Effect of Guest Size on the Oligocholate-Induced Leakage.

Different transport mechanisms are expected to respond very differently to an increase in the guest size. Diffusion of the carrier–guest complex in the membrane slows down as its size

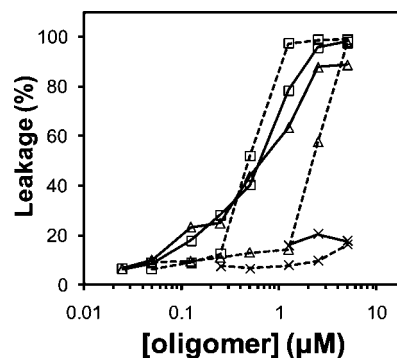


**Figure 4.** Percent leakage of maltotriose at 30 min from POPC/POPG LUVs as a function of oligocholate concentration for **1** (□), **2** (△), and **3** (×) at ambient temperature. The data points connected by solid lines are for maltotriose, whereas those connected by dotted lines are for glucose, taken from Figure 2. Total concentration of phospholipids was 107  $\mu\text{M}$ .

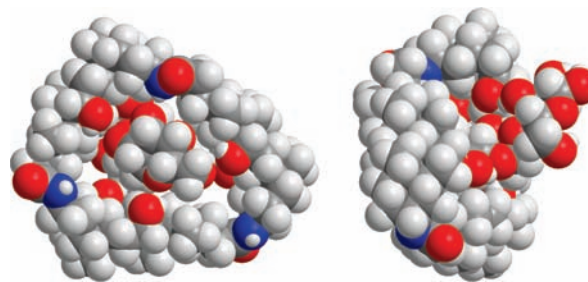


**Figure 5.** Two views of space-filling molecular models of compound **1** with an included maltotriose. The molecular models were generated by Chem3D and optimized with the MM2 force field.

increases. Because it is more difficult for a larger hydrophilic guest to hop from one station to another in a hydrophobic membrane, relay will become less efficient as well. Leakage through a nanopore, on the other hand, should not be affected very much as long as the cross section of the guest is smaller than the pore diameter.

We thus studied the permeation of maltotriose by the cholate macrocycles (Figure 4). Although the trisaccharide is much longer than glucose, its cross section remains the same. Consistent with the pore-formation mechanism, the increase of the sugar size did not slow down the leakage. The  $\text{EC}_{50}$  for the trimer (□) was almost the same for maltotriose ( $\sim 0.6$   $\mu\text{M}$ ) and glucose ( $\sim 0.5$   $\mu\text{M}$ ). Remarkably, tetramer **2** was considerably more effective at leaking the longer sugar; the  $\text{EC}_{50}$  of the tetramer (△) went from 2.4  $\mu\text{M}$  for glucose to  $\sim 0.7$   $\mu\text{M}$  for maltotriose.

Why did the tetramer transport a longer sugar better than a shorter one? The result is highly unusual and contrary to what the diffusion of the guest (inside the pore) would predict. As shown by the molecular models (Figure 5), the trisaccharide is too long to fit within one macrocycle. Hence, as the sugar enters the membrane, it will thread through the macrocycles and template the pore formation. If one assumes that a longer sugar diffuses more slowly than a shorter one inside the pore, the fact that **2** benefited more than **1** in the trisaccharide transport suggests that the template effect was stronger in the tetramer. The conclusion is supported by both the rigidity consideration and the earlier glucose leakage data, which suggest that pore-formation is more difficult with the tetramer. In general, an effect is manifested most strongly where it is most needed. Such a trend is frequently observed

- (33) (a) Demel, R. A.; Bruckdorfer, K. R.; Van Deenen, L. L. *Biochim. Biophys. Acta* **1972**, *255*, 321–330. (b) Papahadjopoulos, D.; Nir, S.; Ohki, S. *Biochim. Biophys. Acta* **1972**, *266*, 561–583.  
 (34) (a) London, E. *Curr. Opin. Struct. Biol.* **2002**, *12*, 480–486. (b) Edidin, M. *Annu. Rev. Biophys. Biomol. Struct.* **2003**, *32*, 257–283. (c) Silvius, J. R. *Biochim. Biophys. Acta* **2003**, *1610*, 174–183. (d) Zhao, J.; Wu, J.; Heberle, F. A.; Mills, T. T.; Klavitter, P.; Huang, G.; Costanza, G.; Feigenson, G. W. *Biochim. Biophys. Acta* **2007**, *1768*, 2764–2776.

in physical organic chemistry—the extent of neighboring group participation, for example, increases with an increase of the electron demand at the reactive center.<sup>35</sup>

Another reason why the tetramer benefited more from the template effect than the trimer could be its larger pore size. According to the molecular model (Figure 5), a sugar fits quite snugly within the inner cavity of **1** and forms multiple hydrogen bonds with the inner wall of the pore. As the sugar gets longer, the number of hydrogen bonds involved would increase, making the passage of the guest more difficult. Hence, the template effect of maltotriose was probably offset by the small pore size of the trimer. For the tetramer, the larger gap between the guest and the pore might have geometrically prohibited the formation of some hydrogen bonds, allowing the trisaccharide to go through the pore with less hindrance.

It should be mentioned that the leakage data with the cholesterol-containing LUVs (Figure 3) or with maltotriose as the guest (Figure 4) did not give the high cooperativity shown in Figure 2. The Hill coefficient ( $n$ ) was only 1–2 in all the cases. The Hill coefficients have been reported to change significantly with minor structural modification of a given system.<sup>29,36</sup> Similar observations were made in biology including in well-established systems such as the hemoglobin–oxygen binding. The reason for the change was not always clear. The Hill equation is known to operate best when extreme positive cooperativity exists between the binding of the first and second molecule.<sup>37</sup> Such a condition may not be met in the glucose transport across the cholesterol-containing hydrophobic membrane or in the maltotriose transport where a template effect is operating.

#### Aggregation of Cyclic Oligocholates Studied by Fluorescence.

Due to its long fluorescence lifetime, pyrene can form excimers quite readily even at relative low concentrations.<sup>38</sup> Aggregation of **4** within a lipid bilayer brings the pyrene groups within proximity and should promote the excimer formation (emitting at 470 nm). Instead of the membrane extrusion method<sup>39</sup> used to prepare the LUVs for the leakage assay, we incorporated the oligocholates into lipid bilayers for dilauroylphosphatidylcholine (DLPC) and POPC/POPG liposomes by the detergent dialysis method. This procedure is often employed to reconstitute membrane proteins into liposomes<sup>40</sup> and has the benefit of generating the most homogeneously mixed lipids. Because cholesterol was found to interfere with the detergent dialysis (possibly because of its strong interactions with the Bio-Beads used in the procedure), we added **4** to preformed LUVs prepared with the membrane extrusion method.

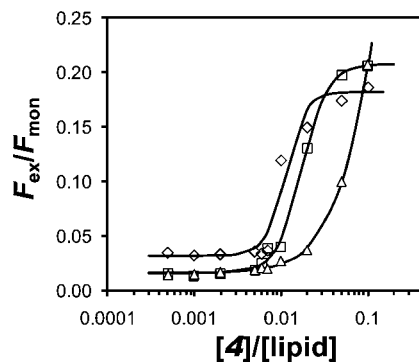


**Figure 6.** The excimer/monomer ratio as a function of [4]/[lipid] ratio in liposomes made of DLPC ( $\Delta$ ), POPC/POPG ( $\square$ ), and POPC/POPG with 30 mol % cholesterol ( $\diamond$ ). The theoretical curves are nonlinear least-squares fitting of the fluorescence data to the Hill equation.

Figure 6 shows the excimer/monomer ratio for compound **4** as a function of the [4]/[lipid] ratio in three different bilayers. Two trends are immediately noticeable. First, the pyrene excimer became stronger as the membrane became more hydrophobic. Among the three bilayers, the C12 DLPC membrane ( $\Delta$ ) was the least hydrophobic and the cholesterol-containing C16–18 POPC/POPG ( $\diamond$ ) the most hydrophobic. With an increase in the membrane hydrophobicity, the inflection point in the excimer/monomer curves, corresponding to the critical aggregation concentration (CAC) of the macrocycle, decreased steadily from 0.02 to 0.01 to 0.007. The trend shows that the formation of pyrene excimer is promoted by membrane hydrophobicity and tracks well with the leakage data. Second, all the excimer/monomer curves were sigmoidal in shape—a hallmark of cooperativity behavior.<sup>41</sup> In fact, when the fluorescence data were fit to the Hill equation, the Hill coefficient ( $n$ ) was  $\sim 1.5$  for the DLPC membrane,  $\sim 3$  for POPC/POPG, and  $\sim 4$  for the cholesterol-containing POPC/POPG. The results showed that the number of the macrocycles in the aggregates correlate with the membrane thickness. The result is in full agreement with our pore-forming mechanism and the leakage data. Because the aggregation is driven by hydrophobic interactions and the pore needs to span the bilayer (to allow water molecules inside the pore to exchange with bulk water), the pore length should not exceed the hydrophobic thickness of the membrane.

#### Conclusions

Classical hydrophobic effect drives the aggregation of hydrophobic molecules in water. By pulling water into lipid bilayers with the amphiphilic cholate macrocycles, we “activated” the water molecules and used them to assemble the macrocycles into transmembrane nanopores.<sup>42</sup> Aggregation and pore-formation seem to be quite efficient for the cyclic tricholate, as it only took 1 macrocycle out of 200 lipid molecules to leak 50% of 300 mM glucose from the LUVs in 30 min. Leakage from the cholesterol-containing LUVs was even more efficient—the same leakage only required 1 macrocycle out of 1000 lipid molecules.

- (35) (a) Lambert, J. B.; Mark, H. W. *J. Am. Chem. Soc.* **1978**, *100*, 2501–2505. (b) Lambert, J. B.; Larson, E. G. *J. Am. Chem. Soc.* **1985**, *107*, 7546–7550.
- (36) (a) Talukdar, P.; Sakai, N.; Sordé, N.; Gerard, D.; Cardona, V. M. F.; Matile, S. *Bioorg. Med. Chem.* **2004**, *12*, 1325–1336. (b) Bhosale, S.; Matile, S. *Chirality* **2006**, *18*, 849–856. (c) Shank, L. P.; Broughman, J. R.; Takeguchi, W.; Cook, G.; Robbins, A. S.; Hahn, L.; Radke, G.; Iwamoto, T.; Schultz, B. D.; Tomich, J. M. *Biophys. J.* **2006**, *90*, 2138–2150. (d) Ferdani, R.; Pajewski, R.; Djedović, N.; Pajewska, J.; Schlesinger, P. H.; Gokel, G. W. *New J. Chem.* **2005**, *29*, 673–680. (e) Chen, W. H.; Shao, X. B.; Regen, S. L. *J. Am. Chem. Soc.* **2005**, *127*, 12727–12735.
- (37) Weiss, J. N. *FASEB J.* **1997**, *11*, 835–841.
- (38) Birks, J. B.; Munro, I. H.; Dyson, D. J. *Proc. R. Soc. London Ser. A* **1963**, *275*, 575–588.
- (39) Olson, F.; Hunt, C. A.; Szoka, F. C.; Vail, W. J.; Papahadjopoulos, D. *Biochim. Biophys. Acta* **1979**, *557*, 9–23.
- (40) Smith, S. A.; Morrissey, J. H. *J. Thromb. Haemost.* **2004**, *2*, 1155–1162.

- (41) Chan, H. S.; Bromberg, S.; Dill, K. A. *Philos. Trans. R. Soc. London B* **1995**, *348*, 61–70.
- (42) For an example of water-promoted assembly in the solid state, see: Carrasco, H.; Foces-Foces, C.; Pérez, C.; Rodríguez, M. L.; Martín, J. D. *J. Am. Chem. Soc.* **2001**, *123*, 11970–11981.

The hydrophobically driven pore-forming mechanism yielded some quite unusual transport properties. Contrary to conventional expectations, permeation of hydrophilic guests occurs more readily as the membrane becomes more hydrophobic and longer sugars passed through the membranes more readily than shorter ones. Transmembrane movement of sugars is accomplished by complex protein transporters in nature,<sup>43</sup> but our oligocholates can be synthesized in a few steps from the cholate monomer.<sup>44</sup> Given the unique pore-forming mechanism, the easy synthesis of the oligocholates, the biocompatibility of cholic

(43) Saier, M. H., Jr. In *The Structure of biological membranes*; Yeagle, P., Ed; CRC Press: Boca Raton, 1992; Chapter 18.

(44) For boronic acid-based sugar transporters, see: (a) Westmark, P. R.; Smith, B. D. *J. Am. Chem. Soc.* **1994**, *116*, 9343–9344. (b) Westmark, P. R.; Gardiner, S. J.; Smith, B. D. *J. Am. Chem. Soc.* **1996**, *118*, 11093–11100.

acid, and the numerous uses of nanopores,<sup>1–9</sup> these compounds may find many applications in biology and chemistry in the future.

**Acknowledgment.** We thank Dr. Xingang Pan for providing compound **1** and performing some initial leakage experiments. We thank NSF (CHE-0748616 and DMR-1005515) for financial support.

**Supporting Information Available:** Experimental Section, including general experimental details, synthesis and characterization of the compounds, leakage assays, and fluorescence experiments. This material is available free of charge via the Internet at <http://pubs.acs.org>.

JA109036Z